Chemical Engineering Journal 161 (2010) 363–370

Contents lists available at ScienceDirect

Chemical Engineering Journal

journal homepage: www.elsevier.com/locate/cej

AlTf-UVM-7—Highly active catalysts for the synthesis of long chain symmetrical ethers and non-ionic surfactant structures

Natalia Candu[a], Mariana Musteata[a], Simona M. Coman[a], Vasile I. Parvulescu[a,*], Jamal El Haskouri[b], Pedro Amoros[b], Daniel Beltran[b]

[a] University of Bucharest, Faculty of Chemistry, Department of Chemical Technology and Catalysis, Bdul Regina Elisabeta 4-12, 030016 Bucharest, Romania
[b] Institut de Ciencia dels Material, Universitat de Valencia E46071, Spain

ARTICLE INFO

Article history:
Received 22 May 2009
Received in revised form 8 October 2009
Accepted 10 October 2009

Keywords:
Bimodal mesoporous structures
Aluminum triflate
Etherification reaction
Symmetrical ethers
Non-ionic surfactants

ABSTRACT

New Lewis acid AlTf-UVM-7 catalysts with bimodal pore system and different Si to Al ratios were prepared in a two-step synthesis in which triflic acid (Tf) was incorporated into previously synthesized mesoporous aluminum-containing silica. The Al incorporation inside the pore walls was carried out through the Atrane method. The characterization of the resulted catalysts showed that the triflic acid treatment step did not damage the texture or the structure of the catalysts. These materials were used as green catalysts for the etherification of fatty alcohols and the conversion of ethylene glycol (EG) with *n*-octanol resulting in mixtures of short ethoxylated structures with a large distribution of C8E1–C8E3 products. The process occurred with high conversions of ethylene glycol and high selectivities to ethoxylated products. Recyclable experiments showed the catalysts are stable and the reuse occurred without changes in the chemical composition.

1. Introduction

For several years there has been a strong trend towards "green" surfactants, particularly for the household sector. Due to their favorable physico-chemical properties, non-ionic surfactants are also extensively used in many fields of technology and research [1–4]. Moreover, non-ionic surfactants are an integral part of the majority of pesticide formulations [5] and of many pharmaceuticals [6].

The mixtures of mono- and di-ethers of corresponding ethylene glycol (EG) are currently used for the preparation of coating solvents, of solvents for paints and of trapping agents for isobutylene from C_4 fraction [7]. Applying the etherification method to obtain such compounds, symmetrical di-ethers can also be formed. They are frequently used in the fine chemical industry for cosmetic products or in the transportation industry as additive for diesel fuels [8].

Preparation of ethers is an important reaction for which a wide variety of procedures have been developed during the last decades. The most commonly used protocol is Williamson ether synthesis [9] which requires initial transformation of alcohols into their corresponding halides or tosylates followed by their displacement with strongly basic alkoxides or phenoxides. Strong basic condition is hazardous to complex molecules carrying base sensitive functional groups. Etherification by direct condensation of alcohols has been considered as an alternative which is conducted in the presence of catalytic amounts of organic or inorganic protic acids [10]. Lewis acids have been also used for direct etherification condensation reactions [11]. In most cases, the reactions suffer from the use of stoichiometric amounts of the Lewis acids which is due to their decomposition by water generated in the process of etherification reactions [11].

A common drawback of the majority procedures applied for the preparation of these valuable compounds is the use of stoichiometric reagents or even conventional homogeneous acid catalysts generating huge amounts of wastes [12]. Therefore, there is a growing need for more environmentally acceptable processes in the chemical industry, e.g., avoiding the use of toxic and/or hazardous substances, using solid acids catalysts instead of homogeneous acids ones. The main procedure in the synthesis of non-ionic surfactants, for example, involves the reaction of primary alcohols with ethylene oxide in the presence of a suitable catalyst [13]. Since ethylene oxide is dangerous both for the human health and environment it is interesting to consider an alternative procedure for their synthesis involving less toxic raw materials. The etherification of glycols with fatty alcohols appears in this context as a solution. Triflic acid (CF_3SO_3H—trifluoromethanesulfonic acid) is known to be a strong acid suitable to be used as catalyst for

* Corresponding author. Tel.: +40 214100241; fax: +40 214100241.
E-mail address: vasile.parvulescu@g.unibuc.ro (V.I. Parvulescu).

1385-8947/$ – see front matter © 2009 Elsevier B.V. All rights reserved.
doi:10.1016/j.cej.2009.10.030

synthetic applications. However, the recovery of the triflic acid from the reaction mixture results in the formation of large amounts of waste. Supported triflic acid is now becoming available to replace homogeneous acid solutions in many organic catalyzed reactions [14–16].

Here we report the surfactant-assisted mesoporous synthesis of heterogeneous Al triflate-silica catalysts, their characterization and the ability of these materials to catalyze the synthesis of ethoxylated chains similar with non-ionic surfactants structures through the etherification of ethylene glycol with primary linear alcohols as 1-octanol, in a greener manner. Moreover, the catalysts are suitable for the production of symmetrical ethers by direct condensation of 1-octanol.

2. Experimental

2.1. The catalysts preparation

The surfactant-assisted mesoporous heterogeneous Al triflate-silica catalysts (denoted as AlTf-UVM-7) were prepared in a two-step synthesis in which the triflic acid was incorporated into previously synthesized Al-containing porous silicas (Al-UVM-7 materials). The first step of the synthesis, carried out using Atrane method [17] produces Al-UVM-7. The general aspects of the procedure for synthesizing UVM-7 material were recently described [18–20]. A typical procedure can be described as follows (Al-UVM-7(25) sample): a mixture of TEOS (32.4 mL, 0.145 mol) and $Al(OBus)_3$ (1.2 mL, 0.005 mol) was slowly added to liquid TEAH3 (70 mL, 0.525 mol), and heated at 150 °C for 10 min to give Atrane complexes. After cooling of the obtained solution at 90 °C, CTABr surfactant (14.2 g, 0.039 mol) was added. After cooling at 60 °C the new solution was mixed with water (243 mL, 13.5 mol) and after few seconds, a white powder appeared. The resulting suspension was allowed to age at room temperature for 4 h. The final (mesostructured) powder was filtered off, washed with water and ethanol, and air-dried. In order to open the pore system, the as-synthesized solid was heated at 550 °C (ramp heating: 1°/min) under static air atmosphere in an electric furnace for 7 h. In all cases, the molar ratio of the reagents in the mother liquor was adjusted to $(2-x)$ Si/x Al/7 TEAH3/0.52 CTABr/180 H_2O (where x = 0.033, 0.043, 0.065 and 0.125). Obtained samples are denoted as Al-UVM-7(y), where y is the Si/Al atomic ratio.

The second step corresponds to the formation of Al-triflate complexes at the Al-UVM-7 surface through heating the Al-containing mesoporous silicas in methanolic solutions of triflic acid. In a representative synthesis 1 g of dried mesoporous aluminosilicate (y = 25; Al-UVM-7(25)) was suspended in a mixture of triflic acid (5 g) and methanol (20 mL). This mixture was stirred under reflux for 4 h at ca. 70 °C. The resulting porous samples were collected by filtration, washed with methanol to eliminate any excess triflic acid, and air-dried. The obtained catalysts were designated AlTf-UVM-7(z), where z is the final Si/Al atomic ratio after reaction with triflic acid.

All the synthesis reagents were analytically pure, and were used as received from Aldrich (tetraethyl orthosilicate [TEOS], aluminum sec-butoxide [$Al(OBus)_3$], triethanolamine [$N(CH_2–CH_2–OH)_3$, hereinafter TEAH3], cetylltrimethylammonium bromide [CTABr], triflic acid, and methanol).

2.2. Catalysts characterization

All obtained materials were characterized using a set of techniques as: electron probe microanalysis (EPMA), X-ray powder diffraction (XRD), nitrogen adsorption–desorption isotherms (−196 °C), transmission electron microscopy (TEM), Fourier transmission infrared spectroscopy (FTIR) and ^{27}Al MAS NMR spectroscopy.

Si, Al, and S elements were analyzed by electron probe microanalysis (EPMA) using a Philips SEM-515 instrument. X-ray powder diffraction (XRD) data were recorded on a Seifert 3000TT θ–θ diffractometer using Cu Kα radiation. Patterns were collected in steps of 0.02° (2θ) over the angular range 1–10° (2θ) for 25 s per step. Transmission electron microscopy (TEM) was carried out with a JEOL JEM-1010 instrument operating at 100 kV and equipped with a CCD camera. Samples were gently grounded in dodecane, and the microparticles were deposited on a holey carbon film supported on a Cu grid. Surface area and pore size values were calculated from nitrogen adsorption–desorption isotherms (−196 °C) recorded on a Micromeritics ASAP-2010 automated instrument. Calcined samples were degassed for 15 h at 130 °C and 10^{-6} Torr before analysis. Surface areas were estimated according to the BET model, and pore size dimensions were calculated using the BJH method. FTIR spectra were collected on a Nicolet 4700 spectrometer (200 scans with a resolution of 4 cm^{-1}) using self-disks of 1% sample in KBr. ^{27}Al and ^{29}Si MAS NMR spectra were recorded on a Varian Unity 300 spectrometer. The MAS probe was tuned at 78.16 and 79.5 MHz for Al and Si nucleus, respectively, and using a magic angle spinning speed of at least 4.0 kHz.

2.3. Catalytic tests

1-Octanol (15 mmol, 1.95 g), and Al triflate-based catalyst (60 mg) was stirred at 150 °C for 2–24 h. After the reaction was stopped, the catalyst was filtered off and the reaction product was analyzed through GC. The products were characterized by GC–MS.

All etherification reactions were done in solvent free conditions, using 15.0 mmol (1.95 g) of 1-octanol as etherification reagent and 60 mg of catalysts; 5.0 mmol of ethylene glycol was used in each reaction (substrate/1-octanol molar ratio = 1/3). Tests were also conducted using a substrate/1-octanol molar ratio of 2/1–1/3. The reaction mixture was kept to 150 °C, for 1–24 h, under strong stirring (1250 rpm) in a 10-mL glass vessel.

After the reaction was stopped, the catalyst was filtered off and the reaction product was analyzed by GC chromatography (Shimadzu GC-2014) and characterized by GC–MS using a Thermo Electron Corporation apparatus.

Recycling tests were carried out as well. After each reaction ended, the catalyst was filtered off, rinsed with methanol and dried under ambient conditions for 2 h. Each catalyst was reused in at least four catalytic cycles. Washed catalysts were analyzed by electron probe microanalysis (EPMA) and FTIR.

3. Results and discussions

3.1. Catalysts characterization

As shown in Section 2, the catalysts were prepared in a two-step synthesis in which the triflic acid was incorporated into previously synthesized mesoporous Al-containing silicas (Al-UVM-7). These structures were built by aggregating nanometric mesoporous particles defining a hierarchic textural-type additional pore system (UVM-7-like materials, a nanometric version of the typical M41 solids). The synthesis strategy has been designed to overcome the problems associated with the reactivity differences between Si and Al species in solution, as well as to favor the stabilization of a bimodal porous system. The first aspect, that frequently leads to chemical inhomogeneous materials and even to phase segregation phenomena, can be easily solved by using the Atrane route as a preparative protocol [17]. This method is based on the use of Atrane complexes (which include triethanolamine-like species as ligands) as hydrolytic precursors.

Table 1
Textural data for Al-UVM-7 and AlTf-UVM-7 porous materials.

Entry	Catalyst	S_{BET} ($m^2\ g^{-1}$)	BJH pore[a] (nm)	Pore volume[a] ($cm^3\ g^{-1}$)	Wall thickness[b] (nm)
1	Al-UVM-7(50)	1170	2.70	2.41	2.15
2	Al-UVM-7(32)	1162	2.68	2.07	2.17
3	Al-UVM-7(25)	1084	2.62	1.55	2.11
4	Al-UVM-7(17)	1042	2.48	1.04	2.02
5	AlTf-UVM-7(71)	1113	2.60	2.00	2.26
6	AlTf-UVM-7(52)	1199	2.58	1.99	2.36
7	AlTf-UVM-7(38)	962	2.52	1.21	2.50
8	AlTf-UVM-7(25)	863	2.33	1.10	2.64

[a] Mesopore diameters and total pore volume calculated by using the BJH model on the adsorption branch of the isotherm.
[b] Pore wall defined as a_0-⌀BJH.

The high accessible bimodal porous (defining large meso-macroporous voids) architecture can be achieved through a quick nucleation process together with a highly suppressed particle growth [18,21,22]. The buffered pH around 9 provided by the TEAH3 seems to be the procedural key for obtaining the bimodal mesoporous system. The resulted catalysts are designated: Al-UVM-7(50), Al-UVM-7(32), Al-UVM-7(25), Al-UVM-7(17), the numbers under brackets representing Si/Al ratio.

For the second synthesis step (consisting of the reaction between accessible Al sites and triflic acid) we have used a preparative protocol adapted from the synthesis method described for Al-triflate complexes in solution [20]. The resulted catalysts are designated: AlTf-UVM-7(71), AlTf-UVM-7(52), AlTf-UVM-7(38), AlTf-UVM-7(25), the numbers under brackets representing Si/Al ratio.

Textural data for all synthesized porous materials are presented in Table 1. As this table shows, increasing the Al content (Si/Al ratio from 50 to 17, for Al-UVM-7 samples, entries 1–4) leads to a progressive decrease in the surface area, mesopore size, the total pore volume and the pore wall. In any case, a high surface area and porosity resulted regardless the aluminum content.

The treatment of these samples with triflic acid provokes an additional reduction in both the mesopore size and the total pore volume (entries 5–8, Table 1). This decrease is basically due to the enhanced nanoparticle packing. On the other hand, the intra-particle mesopore size also decreases with the incorporation of triflate groups. Therefore, as the a_0 parameter remains practically unchanged with the Al and triflate content, the thickness of the pore walls (defined as a_0-⌀BJH pore size) shows a clear tendency to increase with the $Al(OTf)_n$ content (Table 1, entries 5–8), which should be correlated with the relative low S/Al molar ratios observed for Al rich samples. Moreover, the high surface area typical of UVM-7 solids is preserved after the second preparation step. A slight S_{BET} decrease is observed as the Al content increases (from ca. 1100–1200 $m^2\ g^{-1}$ for low Al-containing materials to values around 860 $m^2\ g^{-1}$). This evolution seems to be related with the gradual intra-particle BJH mesopore size decreases and the wall thickness increases.

The symmetry and order degree of the catalysts before and after reaction with triflic acid were studied by XRD and TEM. XRD provides information only on the intra-particle mesopore relative organization (i.e., the surfactant templating pore system). Fig. 1 shows the XRD patterns corresponding to Al-UVM-7 (Fig. 1A) and AlTf-UVM-7 (Fig. 1B) samples. Both materials display XRD patterns in the low-angle region with at least one strong reflection at low 2θ values, which is typical in mesostructured/mesoporous materials. Irrespective of the aluminum content, a similar organization and morphology is achieved for the synthesized Al-UVM-7 samples (Fig. 1A). The representative TEM image (inset in Fig. 1A) clearly shows that the typical UVM-7 architecture based on the aggregation of mesoporous nanoparticles is preserved, in agreement with adsorption–desorption of N_2 isotherms measurements.

Apart from the intense peak at low 2θ values (associated to the (1 0 0) reflection if a hexagonal cell is assumed), a broad signal of

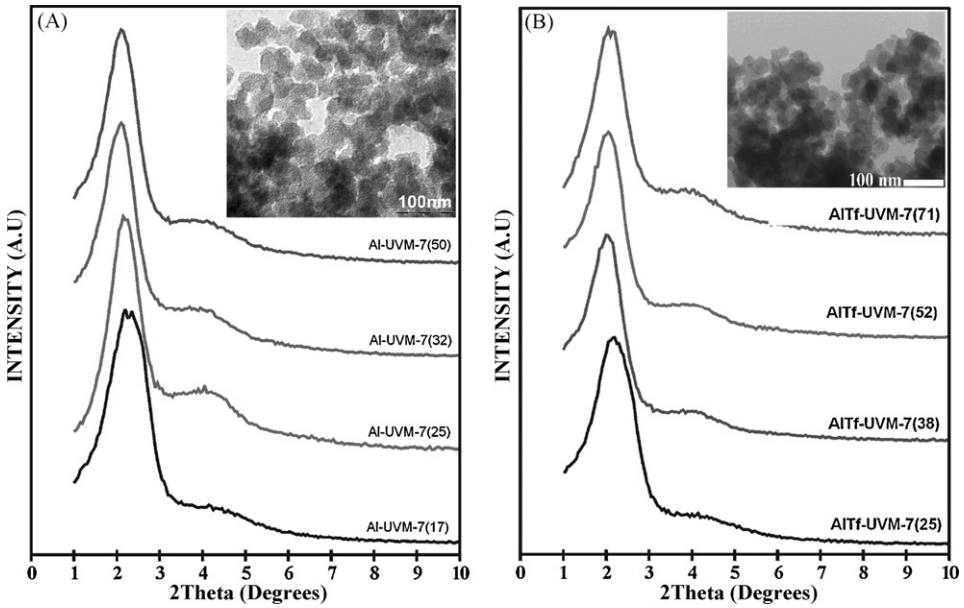

Fig. 1. Low-angle XRD patterns of (A) Al-UVM-7; the inset shows a representative TEM image of the Al-UVM-7 materials corresponding to Al-UVM-7(32) and (B) AlTf-UVM-7; the inset shows a representative TEM image of the Al-UVM-7 materials corresponding to Al-UVM-7(38).

relatively low intensity that can be indexed to the overlapped (1 1 0) and (2 0 0) reflections of the typical hexagonal cell. The detection of this last unresolved broad signal is typical of hexagonal disordered mesopore arrays.

The relative intensity of this signal remains practically unchanged for samples in the molar range, and is slightly decreased for the Al-UVM-7(17) sample. This tendency indicates that the incorporation of large Al amounts in the silica-based mesoporous framework implies a lowering of the order in the pore array. The lattice parameter value remains practically unchanged and only a small and progressive shrinkage is observed as the Al content increases.

The intra-particle mesopore system in AlTf-UVM-7 catalysts also maintains the hexagonal disordered symmetry (Fig. 1B). A practically constant lattice parameter value ($a_0 = 4.94 \pm 0.08$ nm) was measured for all samples in the chosen compositional range. Irrespective of the Al and triflate content, the preservation of the UVM-7 architecture is also confirmed by the TEM images (inset in Fig. 1B).

The TEM images completely correlated with the XRD observations. Typical morphologies – hexagonal ordered large particles and aggregates of disordered nanoparticles – were observed both for Al-UVM-7 and AlTf-UVM-7 samples. Moreover, the TEM images allow the establishment of a certain tendency in the variation of both the particle size and the progress of the cluster-like aggregation with the Al and triflate content. Thus, the average particle size slightly decreases as the Al content increases (from ca. 45 to 29 nm). The progressive Al and triflate incorporation also favors the formation of denser aggregates, reflecting a more efficient packing of the primary nanoparticles, in agreement with the textural results. Such an evolution of the mesostructure can be firstly related to the attack of triflic acid activating the silica surface of the nanoparticles, and thus favoring the subsequent inter-particle condensation through the formation of Si–O–Si bonds. Moreover, the ability of the Al atoms to increase their coordination number favors the inter-particle connectivity through (additional) Al–O–Al or Al–O–Si links.

3.1.1. *The chemical properties of the catalysts*

Except Al-UVM-7(17) sample, the Si/Al molar ratio in the final solid is lower than that in the mother solution (Table 2). The increased Si/Al ratio, compared with the values of mother solution, became even more prominent in the case of the AlTf-UVM-7 samples (Table 2, entries 5–8). As we previously showed for Zr-UVM-7 materials [20], this effect could be associated with the comparatively low solubility of the Al-containing species with regard to the pure silica ones.

This tendency should decrease as the amount of well-dispersed Al sites increase. In spite of this, there is no significant preferential incorporation of Al or Si into the final network. This result is a consequence of the harmonization of the hydrolytic reaction rates of the Si and Al species when starting from Atrane precursors instead of conventional alkoxides. EPMA analysis shows that all Al-UVM-7 samples are chemically homogeneous with a regular distribution of aluminum and silicon atoms throughout the inorganic walls at the micrometer level (spot area ≈ 1 μm) (Table 2). Hence, the solids can be considered as monophase products.

Table 2
Synthetic data for Al-UVM-7 and AlTf-UVM-7 porous materials obtained from EPMA measurements.

Entry	Catalyst	Si/Al/*x*	Si/Al/*y*	Si/Al/*z*	S/Al
1	Al-UVM-7(50)	60	50	–	–
2	Al-UVM-7(32)	45	32	–	–
3	Al-UVM-7(25)	30	25	–	–
4	Al-UVM-7(17)	15	17	–	–
5	AlTf-UVM-7(71)	50	–	71	0.9
6	AlTf-UVM-7(52)	32	–	52	0.9
7	AlTf-UVM-7(38)	25	–	38	0.8
8	AlTf-UVM-7(25)	17	–	25	0.6

Where *x* is the Si/Al atomic ratio in the mother liquor, *y* is the Si/Al atomic ratio in the aluminum-based samples, *z* is the final Si/Al atomic ratio after reaction with triflic acid.

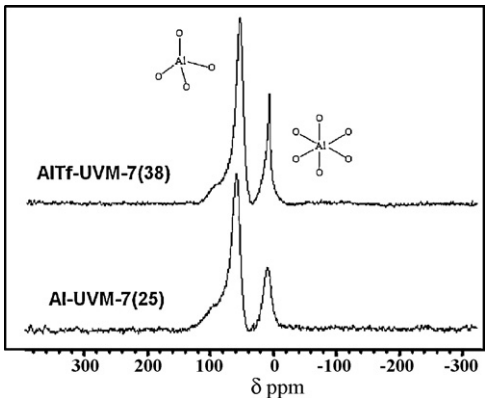

Fig. 2. ^{27}Al NMR MAS spectra of Al-UVM-7 and AlTf-UVM-7 samples.

The second reaction step occurs with a significant Al leaching (30–35%) according to EPMA measurements (Table 2, entries 5–8). The similar loss of Al atoms regardless the Si/Al ratio can be due to the fact that an identical large amount of triflic acid (in excess) has been used for the preparation of AlTf-UVM-7(71)–AlTf-UVM-7(25) samples.

Representative ^{27}Al NMR MAS spectra are displayed in Fig. 2. All samples show, before and after the second preparative step, similar ^{27}Al NMR MAS spectra with an averaged ratio of Al(Td):Al(Oh) = 60:40. Therefore, we can suppose that the included triflate ligands must be preferably coordinated around the 40% of octahedral Al atoms.

A bimodal attack to the catalyst surface can be attributed to the triflic acid: (1) the typical rupture of Si–O–Si or Si–O–Al bonds due to the apparent (in methanol) acid media, and (2) a preferred attack to accessible Al sites to form aluminum-triflate complexes. In fact, a certain proportion of the leached Al atoms is probably extracted from the mesoporous materials as triflate complexes in solution during the washing process with methanol. In the case of the Si atoms, a significantly lower leaching is expected taking into account the unfavorable formation of triflate complexes when compared to Al sites. In this case, the possible low Si atom evolution must be viewed as a subsequent effect of the dealumination process. Hence, the silica network before and after the triflic acid treatment remains practically unchanged according to ^{29}Si NMR MAS spectra showed in Fig. 3: both samples display a strong signal centered at ca. −107 ppm attributed to a mixture of Q^4 and Q^3 silanol groups. The low intensity and broad signal observed at ca. −75 to −80 ppm for the AlTf-UVM-7(38) should be assigned to unusual isolated Q^1 silanol groups generated through the dealumination process. This observation would be considered as a probe on the possible Si small leaching mechanism.

Apparently, the proportion of included triflate groups is very low and follows an *a priori* unexpected tendency contrary to the amount of Al. In fact, the maximum triflate/Al molar ratio corresponds to 0.9 (AlTf-UVM-7(71)), and progressively decreases as the Al content increases up to values around 0.6 (Table 2, entries 5–8).

Fig. 4 gives more evidences on the formation of the Al triflate species. FTIR spectra indicate that the UVM-7 support did not retain even a trace of triflate. In contrast, on doped Al-silica samples, triflic acid is incorporated in amounts that increase with increasing the proportion of accessible Al atoms. The spectra of AlTf-UVM-

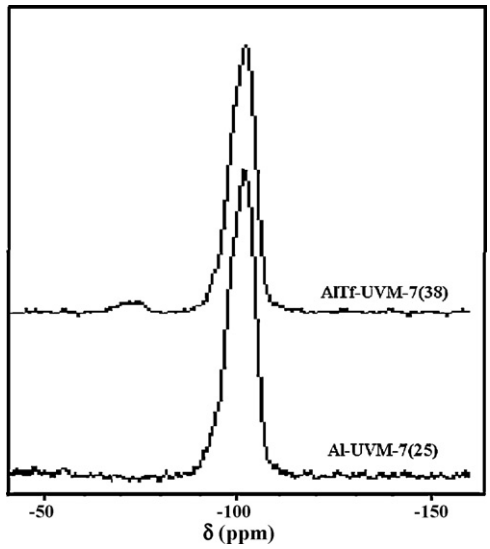

Fig. 3. ^{29}Si NMR MAS spectra of Al-UVM-7(25) and AlTf-UVM-7(38) samples.

7(38) and AlTf-UVM-7(25) samples show small additional bands (which are absent in the spectrum of Al-UVM-7(38) sample) at 1294–1185 and 600 cm^{-1} that can be assigned to S=O stretching vibrations and deformation modes of SO_2 moieties, respectively [23,24]. In spite of the Al leaching during the second reaction step, this post-treatment with triflic acid does not modify the mesostructure previously described for Al-UVM-7 samples.

3.1.2. The stoichiometry of the active sites

It is necessary to consider that only a certain proportion of Al sites are located at the surface and the remaining Al atoms, inside the pore walls, never can be accessible to the triflate ligands. Hence, we can assume that majority of non-accessible Al sites should correspond to framework aluminum with tetrahedral coordination environments, and the Al sites more favorable to be attacked by triflate ligands should be those at the surface with expanded octahedral coordination. These last Al centers complete their coordination environment with more labile OH– and H_2O ligands, when compared to the oxygen atoms of the silica framework. Therefore, ^{27}Al NMR spectra of the samples before and after reaction with triflic acid can provide useful information to estimate the proportion of accessible Al atoms and to propose a formulation for the active $Al(OTf)_n$ sites.

Under this reasonable hypothesis, the stoichiometry of the active $Al(OTf)_n$ sites at the silica surface is comprised in the range $Al(OTf)_{2.4}$ to $Al(OTf)_{1.7}$ for AlTf-UVM-7(71) and AlTf-UVM-7(25), respectively. Then, the 1:2 complex ($Al(OTf)_2$) seems to be the predominant specie for all synthesized catalysts. The decrease in the n value as the Al amount increases could be tentatively attributed to the progressive increase of the pore wall thickness and the subsequent relative increase of non-accessible Al sites.

Based on the physical–chemical characterization results, a general picture of the prepared materials can be schematically depicted as follows (Scheme 1).

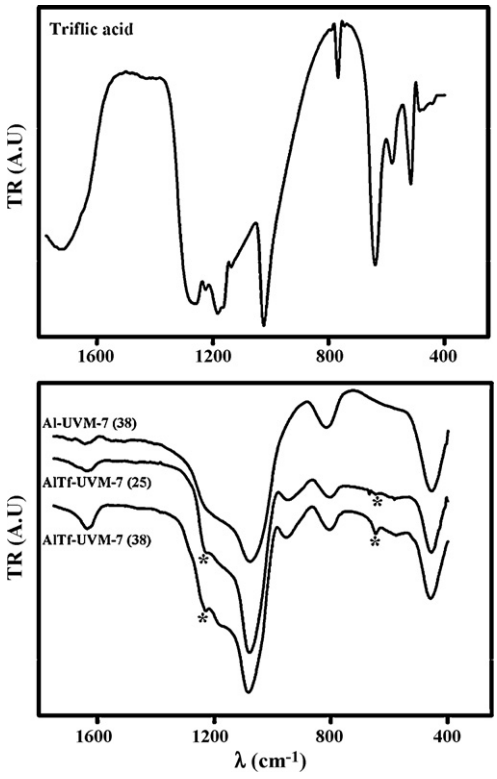

Fig. 4. IR spectra of Al-UVM-7(38), AlTf-UVM-7(38) and AlTf-UVM-7(25) samples compared with the IR spectrum of triflic acid in aqueous solution.

3.2. Catalytic tests

Mesostructured AlTf-based catalysts were primarily assessed in the etherification of 1-octanol, a reaction relevant for the synthesis of emulsifiers for cosmetic applications and of additives for diesel fuels (Scheme 2). The relatively large molecular size of the reactant (1-octanol) and product (dioctyl ether) makes them more readily manageable over catalytic materials within the mesoporous range of pore size, in comparison with a more traditional acid-based catalyst such as microporous zeolites (e.g., BEA zeolite [25]).

The reaction proceeded smoothly and produced dioctyl ether (DOE) in the 25.0–72.0% range, after 24 h, as a function of the catalyst texture. In the presence of Al-UVM-7 catalysts, the highest yield to DOE was obtained in the presence of Al-UVM-7(50) sample (45.1%), characterized by the lowest amount of aluminum. The presence of the $Al(OTf)_2$ sites on the surface of AlTf-UVM-7 samples contribute to the increase in the yield of DOE. On all AlTf-UVM-7 catalysts series, the obtained yield to DOE was higher than that on the Al-parent samples. Again, the highest yield to DOE (71.8%) was obtained on the sample characterized by the lowest amount

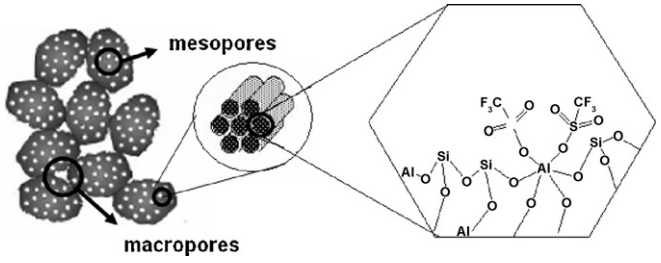

Scheme 1. The schematic representation of the active sites.

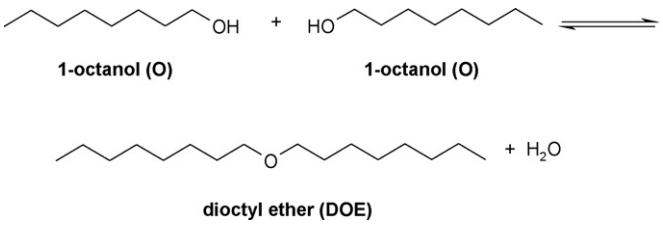

Scheme 2. Etherification of 1-octanol to dioctyl ether (DOE).

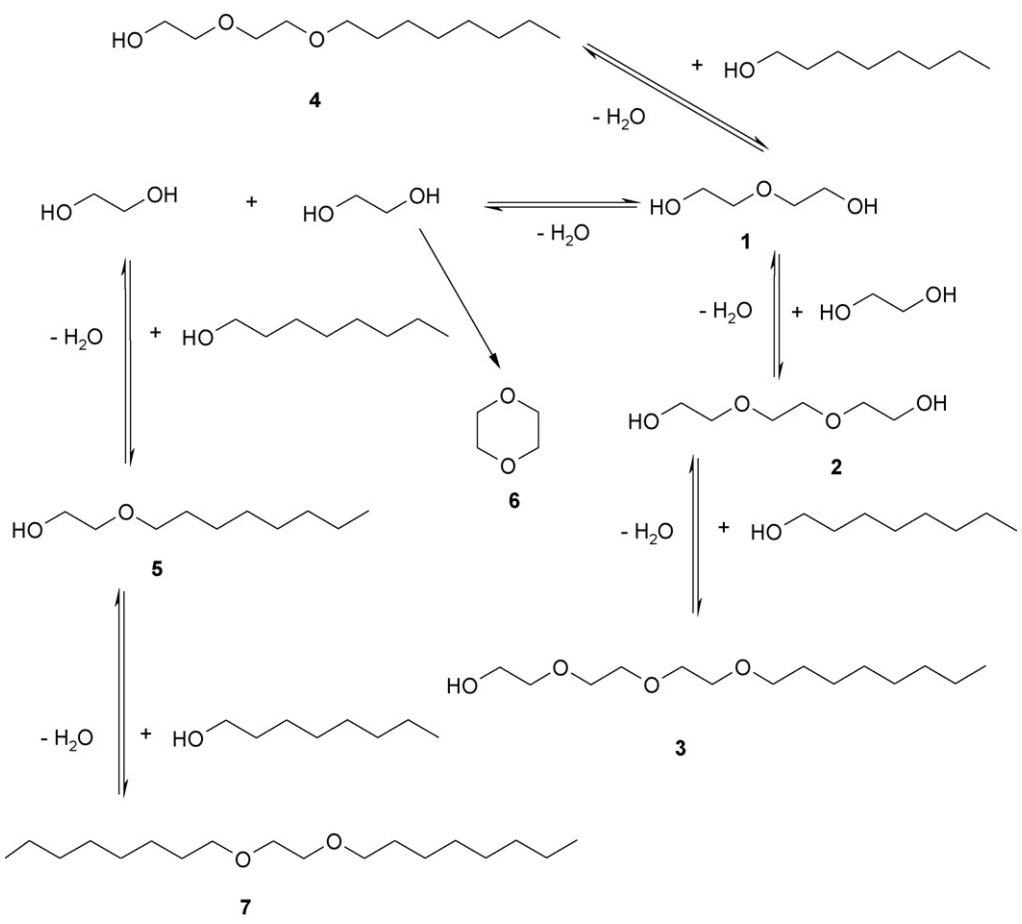

Scheme 3. Possible reaction pathways in the etherification of ethylene glycol (EG) with 1-octanol (O).

of aluminum and the higher density of strong $Al(OTf)_2$ sites (AlTf-UVM-7(71)).

Mesostructured AlTf-UVM-7 catalysts were then tested in the etherification of ethylene glycol with 1-octanol. This acid catalyzed reaction has been chosen as an another appropriate example due to the high added value of the produced compounds, with typical structure of non-ionic surfactants. The etherification of ethylene glycol with 1-octanol is a complex of acid catalyzed consecutive equilibrium reactions (Scheme 3).

The relatively large molecular size of the reactants and products makes them more readily manageable over catalytic materials within the mesoporous and/or macroporous range, in comparison with a more traditional acid-based catalyst [26].

Throughout this text fatty alcohol ethoxylates are referred to as C_mE_n, with m being the number of carbon atoms in the alkyl chain and n being the number of oxyethylene units.

While the conversion of EG was very high (>97%) irrespective of the Si/Al molar ratio and the density of $Al(OTf)_2$ acid sites, this time 1-octanol was transformed only in a low degree (3–35%) (Fig. 5a). In a similar way with the condensation of 1-octanol reactions the highest conversion of 1-octanol was obtained in the presence of AlTf-UVM-7(71), characterized by the lowest amount of aluminum in the structure network and the highest density of $Al(OTf)_2$ acid sites. The higher conversion of EG can be due to its higher dielectric constant (37.0, 50 °C) in comparison with that of 1-octanol (10.3, 50 °C) and to the strong competitive adsorption between these two molecules for active sites.

The efficiency of the catalysts has been checked in recyclable experiments. The leaching test carried along these experiments showed that, indeed, the mesostructured AlTf samples correspond

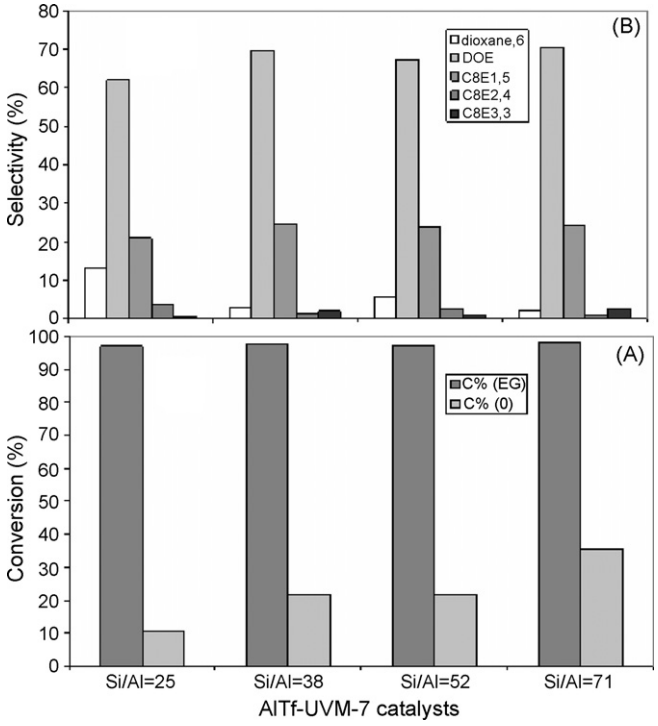

Fig. 5. (A) The variation of the EG and 1-octanol conversion and (B) the distribution of the reaction products as a function of the Si/Al molar ratio (EG/O = 0.3, 150 °C, 24 h).

to stable catalysts. After the separation of the mother liquor neither the level of the glycols conversion nor the products distribution has changed for another 4 h. On the other side, chemical analysis carried out by EPMA, indicated no change in the catalyst composition. It can be thus concluded that these catalysts are stable under the reaction conditions, and the reaction takes place under heterogeneous conditions. Moreover, the catalysts showed a high activity (>90%) for at least three cycles. Unfortunately, after more cycles the activity slowly starts to decrease (ca. 10%) and this decrease was accompanied by a change in the products distribution. This decrease in the catalyst activity and the modification in the reaction products distribution is likely related to the physical blockage of the very active sites by organic compounds.

It is well known that ethoxylated surfactants can be tailor-made with high precision with regard to the average number of oxyethylene units added to a specific hydrophobe, e.g., a fatty alcohol [26]. However, the ethoxylation invariably gives a broad distribution of chain lengths. If all hydroxyl groups, i.e., those of the starting alcohol and the glycol ethers formed, exhibit the same reactivity, a Poisson distribution of oligomers would be obtained.

Since the starting alcohol is slightly less acidic than the ethylene glycol, its deprotonation is disfavored, leading to a lower probability for reaction with ethylene glycol. Hence, a considerable amount of unethoxylated alcohol will remain in the reaction mixture, also with relatively long ethoxylates chain. This is sometimes a problem and considerable efforts have been made to obtain a narrower homologue distribution.

Applying the etherification of EG with 1-octanol as methodology for the synthesis of ethoxylated surfactants, the distribution of the reaction products varies as a function of the active species in catalytic samples (Fig. 5b). Therefore, all catalysts favor the "self" etherification of 1-octanol to DOE (di-octanol ether), followed by the condensation of EG with 1-octanol to C8E1 product. C8E3 was obtained only in very low amounts, in the presence of AlTf-UVM-7 catalysts (Fig. 5b). Again, the obtained results can be correlated with the strength of the acidic sites, the stronger ones favoring the condensation of the EG with the fatty alcohol.

The effect of the variation of the molar ratio of EG to 1-octanol was studied from 2:1 to 1:3 mol under otherwise similar conditions, in the presence of AlTf-UVM-7(25) catalyst (Fig. 6). The conversion of ethylene glycol increased from 83.8 to 97.1% as the molar ratio of EG to 1-octanol decreased from 2 to 0.3. On the other hand, when the initial 1-octanol concentration was five times higher (EG/O = 0.3 instead 2) the conversion of 1-octanol was approximately three times lower (10% instead of 29%). So, when the catalyst surface is fully covered with alcohol the reaction rate is lower than in the case

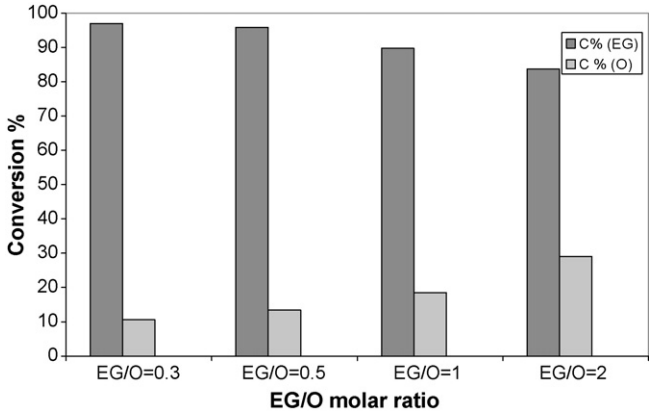

Fig. 6. The influence of the EG/O molar ratio upon the activity of the AlTf-UVM-7 (Si/Al = 25) catalyst (150 °C, 24 h).

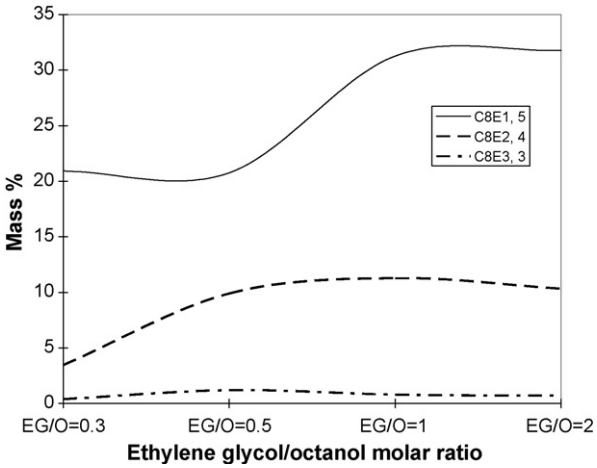

Fig. 7. The influence of the EG/O molar ratio upon the distribution of the reaction products in the presence of the AlTf-UVM-7 (Si/Al = 25) catalyst (150 °C, 24 h).

of a partially covered catalyst surface. This indicates some kind of inhibiting effect of the reactant itself, i.e., the 1-octanol, than an inhibition of EG.

A similar behavior was observed by Françoise and Thyrion for the ethanol in the synthesis of ethyl tert-butyl ether catalyzed by Amberlyst-15 [27]. They ascribed this to the occurrence of two different mechanisms depending on the concentration of ethanol. At a high ethanol concentration the acid sites would become solvated, i.e., weaker acid sites.

Peaked ethoxylates have a growing share of the market. Typical advantages of ethoxylates with peaked distribution are: (i) the low content of free alcohol reduces smell; (ii) the low content of free alcohol reduces "pluming" during spray-drying; (iii) the low content of low oxyethylene homologues increases solubility; (iv) the low content of high oxyethylene homologues reduces viscosity [26]. Regarding the products distribution, it seems that this process can only be used to prepare short ethoxylated structures (Fig. 7).

On the other hand, the process occurs with the formation of a large spectrum of ethoxylated products, a mixture of C8E1–C8E3 in different ratios as a function of the Si/Al ratio and the density of accessible acid sites. Unfortunately, this is a disadvantage of the applied process.

4. Conclusions

The data obtained in this study demonstrates that in the investigated AlTf-UVM-7 catalysts, triflate is associated with well-dispersed hexacoordinated Al species. The synthesis of these catalysts was achieved in two steps, with triflic acid incorporated into previously synthesized mesostructured Al-containing silicas. The characterization of the resulted catalysts showed that this step did not damage the texture or the structure of the catalysts. These new materials were used as green catalysts for the conversion of ethylene glycol (EG) and *n*-octanol to the corresponding ethoxylated chain similar with non-ionic surfactants structures. Reaction occurs with high ethylene glycol conversions. Unfortunately, the distribution of these ethoxylated products is too large to represent an advantage as non-ionic surfactant structures. Moreover, the process occurs with the formation of short ethoxylated structures. The applied catalytic systems are more suitable for the production of symmetrical long chain ethers. With all these, the process can constitute a base for the development of new greener synthetic procedures in the preparation of non-ionic surfactants.

Acknowledgements

This research was supported by the CNCSIS (PNCDI II 40/2007) and the MICIIN (MAT2003-08568-C03-01 and MAT2009-14564-C04-04).

References

[1] I.Y. Galaev, B. Mattiasson, Thermoreactive water-soluble polymers, nonionic surfactants, and hydrogels as reagents in biotechnology, Enzyme Microb. Technol. 15 (1993) 354.
[2] S. Lennie, P.J. Hailing, G. Bell, Causes of emulsion formation during solvent extraction of fermentation broths and its reduction by surfactants, Biotechnol. Bioeng. 35 (1990) 948.
[3] G.J. Piazza, Lipoxygenase catalyzed hydroperoxide formation in microemulsions containing nonionic surfactant, Biotechnol. Lett. 14 (1992) 1153.
[4] S.S. Helle, S.J.B. Duff, D.G. Cooper, Effect of surfactants on cellulose hydrolysis, Biotechnol. Bioeng. 42 (1993) 611.
[5] D. Seaman, Trends in the formulation of pesticides—an overview, Pestic. Sci. 29 (1990) 437.
[6] J.E. Fontan, P. Arnaud, J.C. Chaumel, Enhancing properties of surfactants on the release of carbamazepine from suppositories, Int. J. Pharm. 73 (1991) 17.
[7] S.S. Jayadeokar, M.M. Sharma, Ion exchange resin catalysed etherification of ethylene and propylene glycols with isobutylene, React. Polym. 20 (1993) 57.
[8] G.A. Olah, T. Shamma, G.K. Surya, Dehydration of alcohols to ethers over Nafion-H, a solid perfluoroalkanesulfonic acid resin catalyst, Catal. Lett. 46 (1997) 1.
[9] A.W. Williamson, On etherification, J. Chem. Soc. 4 (1852) 229.
[10] M.B. Smith, J. March, Advanced Organic Chemistry, fifth ed., Wiley/Interscience, New York, 2001.
[11] S. Kim, K.N. Chung, S. Yang, Direct synthesis of ethers via zinc chloride-mediated etherification of alcohols in dichloroethane, J. Org. Chem. 52 (1987) 3917.
[12] A. Behr, L. Obendorf, Development of a process for the acid-catalyzed etherification of glycerine and isobutene forming glycerine tertiary butyl ethers, Eng. Life Sci. 2 (2002) 185.
[13] H.F. Drew, J.R. Schaeffer, Ethylene oxide addition to long-chain alcohols, Ind. Eng. Chem. 50 (1958) 1253.
[14] S.M. Coman, G. Pop, C. Stere, V.I. Parvulescu, J. El Haskouri, D. Beltrán, P. Amorós, New heterogeneous catalysts for greener routes in the synthesis of fine chemicals, J. Catal. 251 (2007) 388.
[15] L.R. Pizzio, Synthesis and characterization of trifluoromethanesulfonic acid supported on mesoporous titania, Mater. Lett. 60 (2006) 3931.
[16] D.O. Bennardi, G.P. Romanelli, J.C. Autino, L.R. Pizzio, Trifluoromethanesulfonic acid supported on carbon used as catalysts in the synthesis of flavones and chromones, Catal. Commun. 10 (2009) 576.
[17] S. Cabrera, J. El Haskouri, C. Guillem, J. Latorre, A. Beltrán, D. Beltrán, M.D. Marcos, P. Amorós, Generalised syntheses of ordered mesoporous oxides: the atrane route, Solid State Sci. 2 (2000) 405.
[18] J. El Haskouri, J.M. Morales, D. Ortiz de Zaĭrate, L. Fernaĭndez, J. Latorre, C. Guillem, A. Beltraĭn, D. Beltraĭn, P. Amoroĭs, Nanoparticulated silicas with bimodal porosity: chemical control of the pore sizes, Inorg. Chem. 47 (2008) 8267.
[19] D. Ortiz de Zarate, A. Gomez-Moratalla, C. Guillem, A. Beltran, J. Latorre, D. Beltran, P. Amoros, High-zirconium-content nano-sized bimodal mesoporous silicas, Eur. J. Inorg. Chem. (2006) 2572.
[20] D.B.G. Williams, M. Lawton, Aluminium triflate: a remarkable Lewis acid catalyst for the ring opening of epoxides by alcohols, Org. Biomol. Chem. 3 (2005) 3269.
[21] J. El Haskouri, D. Ortiz de Zarate, C. Guillem, J. Latorre, M. Caldes, A. Beltran, D. Beltran, A.B. Descalzo, G. Rodriguez, R. Martinez-Mañez, M.D. Marcos, P. Amoros, Silica-based powders and monoliths with bimodal pore systems, Chem. Commun. (2002) 330.
[22] L. Huerta, C. Guillem, J. Latorre, A. Beltran, R. Martinez-Mañez, M.D. Marcos, D. Beltran, P. Amoros, Bases for the synthesis of nanoparticulated silicas with bimodal hierarchical porosity, Solid State Sci. 8 (2006) 940.
[23] L.J. Bellamy (Ed.), The Infrared Spectra of Complex Molecules, Wiley, New York, 1960.
[24] M. Chidambran, C. Venkatesan, P.R. Rajamohanan, A.P. Singh, Synthesis of acid functionalized mesoporous $\equiv Zr\cdots O\cdots SO_2\cdots CF_3$ catalysts; heterogenization of CF_3SO_3H over mesoporous $Zr(OH)_4$, Appl. Catal. A: Gen. 244 (2003) 27.
[25] I. Hoek, T.A. Nijhuis, A.I. Stankiewicz, J.A. Moulijn, Kinetics of solid acid catalysed etherification of symmetrical primary alcohols: zeolite BEA catalysed etherification of 1-octanol, Appl. Catal. A: Gen. 266 (2004) 109.
[26] K. Holmberg, B. Jönsson, B. Kronberg, B. Lindman, Surfactants and Polymers in Aqueous Solution, second ed., John Wiley & Sons, Ltd., 2003.
[27] O. Françoise, F.C. Thyrion, Kinetics and mechanism of ethyl *tert*-butyl ether liquid-phase synthesis, Chem. Eng. Process 30 (1991) 141.